Power Improvement of Non-Linear Wind Turbines during Partial Load Operation using Fuzzy Inference Control

Hamed Habibi*, Aghil Yousefi Koma, Ian Howard*****

**PhD, Faculty of Science and Engineering, School of Civil and Mechanical Engineering, Curtin University, Perth, Australia (e-mail: hamed.habibi@postgrad.curtin.edu.au)*
***Professor, Centre of Advanced Systems and Technologies (CAST), School of Mechanical Engineering, College of Engineering, University of Tehran, Tehran, Iran (e-mail: aykoma@ut.ac.ir)*
**** Professor, Faculty of Science and Engineering, School of Civil and Mechanical Engineering, Curtin University, Perth, Australia (e-mail: i.howard@curtin.edu.au)*

Abstract: Power generation in modern and industrial wind turbines can be improved by careful choice and analysis of operational control strategies. In this paper a new controller scheme is proposed in partial load operation of the wind turbine where the pitch angle is kept constant at zero and the generator torque is adjusted utilizing the fuzzy inference method. Fuzzy rules were defined with respect to the response of the wind turbine to reference gains such that the output power tracks the ideal power curve as close as possible without any significant increase of stress on the main shaft and drive train. A variety of membership shape functions were considered to show the resulting effect on the extracted energy and the drive train stress. Accordingly, through numerous simulations, it can be seen that the total harvested energy is increased. The fuzzy controller was evaluated based on a nonlinear model of the wind turbine using real wind speed applied to the model as a disturbance, to consider the practicality of the proposed controller.

Keywords: Fuzzy inference system, Wind turbine Model, Partial load operation, Power Extraction.

1. INTRODUCTION

Wind turbines are used to harvest the kinetic energy available in the wind as electrical energy, and are one of the most reliable and sustainable forms of renewable energy. The modern industrial wind turbines are equipped with longer blades, higher towers and, to have more uniformly available wind speed, are installed in remote locations. These issues require the need for modern control strategies to be considered to increase the harvested wind energy whilst keeping the structural load at a desirable level to decrease maintenance costs (Sloth et al., 2009).

The wind energy is transferred to the wind turbine by rotating the wind turbine blades which are coupled to the generator shaft. Generally, the wind turbine is highly nonlinear due to its aerodynamic characteristics which can be represented as a function of blade pitch angle, rotor rotational speed and wind speed. Consequently, the aerodynamic torque and thrust are being exerted onto the rotor and the tower, respectively. The rotational speed of the generator is increased by utilizing a high speed ratio drive train (Bianchi et al., 2006). It should be noted that this paper utilises a wind turbine model with variable speed-variable pitch that can operate over a wider range of wind speeds.

In Figure 1, a typical ideal power curve is shown in which P_a is the ideal generated power and v_w is the wind speed applied at the rotor plane. Indeed, this curve can be seen as the desirable one to be tracked by the wind turbine (Bianchi et al., 2006). Cut-In wind speed, i.e. $V_{W,cut-in}$, represents the lowest practical operational wind speed and Cut-Out wind speed, i.e. $V_{W,cut-out}$, is the highest wind speed for wind turbine operation and the wind turbine is shut down for wind speeds out of this range (Esbensen et al., 2008). The operational regions of wind turbines can be considered into two regions. The first region so-called partial load operation, is between the Cut-In wind speed, where wind turbine starts to work, and the wind speed at where the wind turbine produces its designated rated power, $P_{a,N}$, is called nominal wind speed, $V_{W,N}$. The full load operation is the region between the nominal wind speed and the Cut-Out wind speed. In partial load operation, the main control goal is to harvest as much energy as possible from the wind speed. This region is called the power optimization region in the literature (Habibi et al., 2016).

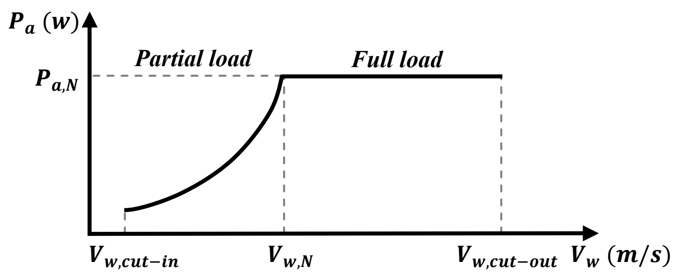

Fig. 1. The ideal power curve.

One of the simplest and therefore most applicable control schemes for wind turbines at partial load operation is to design PID controllers for a set of linearized wind turbine models at different operating points and scheduling between these controllers (Esbensen et al., 2008; Hammerum, 2006; Laks et al., 2009).

The disadvantages of this scheme is the resulting instability that occurs at transition steps between different controllers. The controllers are often designed based on linearized models which also decreases the controller efficiency on nonlinear wind turbine models (Lajouad et al., 2014).

The most commonly used controller, also known as the reference controller in previous research, is the standard control law that is obtained by excluding the wind speed in the aerodynamic torque equation (Johnson et al., 2006). In this paper the standard control law is chosen to be the reference controller for the wind turbine operation providing a reference for comparison of results obtained using the fuzzy control.

The use of fuzzy logic and fuzzy inference analysis in control continues to grow. (Badihi et al., 2014) studied the fuzzy PI controller for gain scheduling basis to remove the fault effects on wind turbines. In similar research, (Aissaoui et al., 2013) tried to extract the maximum wind power by focusing on the electrical dynamics of the generator by using fuzzy PI control. (Lakhal et al., 2015), maximised the total power of the linearized wind turbine model, using fuzzy control, by feeding the wind speed and generator speed to the controller. (Bououden et al., 2013) introduced fuzzy model predictive control using linear matrix inequality to control the linearized wind turbine.

(Gao et al., 2008) focussed on controlling the blade pitch angle using a PI fuzzy controller. Similarly, (Jian-Jun et al., 2010) considered the effect of using variable blade pitch on the wind turbine with fuzzy logic. (Ata and Koçyigit, 2010) predicted the power coefficient and tip speed ratio, utilizing an adaptive neuro-fuzzy inference system. (Qi and Meng, 2012) through a linearized model of the wind turbine, proposed a controller for the blade pitch angle using fuzzy logic and PID control. (Bedoud et al., 2015) tuned the gains of a PI controller based on an adaptive fuzzy scheme to control the generator of a linear wind turbine model. (Shamshirband et al., 2014), looked at maximizing the wind farm profit and designed an optimization procedure based on adaptive neuro-fuzzy inference system.

The main contribution of the current paper in comparison to previous research is that a fuzzy inference system is used in this paper to adjust the gains of the reference controller that is implemented on a nonlinear model of wind turbine whose main objective is operating closely to ideal power curve. The fuzzy inference system uses the generator speed and its rate to determine appropriate gains according to fuzzy laws. In addition, the overall stress on the drive train is considered as a control objective as well as the captured energy. On the other hand, the wind is usually considered as a disturbance in the proposed controller scheme, as it is not possible to be measured accurately at the rotor plane and is known to have non-uniform transient characteristics across the rotor. Several fuzzy membership functions are considered to study their effect on the resulting extracted energy and for further analysis. The final proposed controller is tested with a real wind speed scenario to check its applicability.

The organization of this paper is as follows. In section 2, the wind turbine model is described in detail. The control strategies for both reference and fuzzy controller are considered and simulated in sections 3 and 4, respectively. The conclusions and final analysis are presented in section 5.

2. WIND TURBINE MODEL

A nonlinear model of a 4.8MW wind turbine is considered for evaluating the proposed controller (Esbensen et al., 2008). The model parameters are available in the Appendix.

2.1. Aerodynamic Model

The rotor shaft speed, $\omega_r(t)$, depends on the available energy in the wind. The air density, ρ, covered area by blades, A and power coefficient, $C_P(\lambda(t),\beta(t))$ are the parameters that affect the final extracted power. C_P depends on the blade pitch angle, $\beta(t)$ and tip-speed ratio, $\lambda(t)$, which is the ratio of blade speed and wind speed (Esbensen et al., 2008). The aerodynamic torque applied on the rotor shaft is as follows.

$$T_a(t) = \frac{1}{2\omega_r(t)}\rho A V_\omega^3 C_P(\lambda(t),\beta(t)) \qquad [Nm] \quad , \qquad \lambda = \frac{\omega_r.R}{V_\omega} \tag{1}$$

where $T_a(t)$ and V_ω are aerodynamic torque and wind speed, respectively. It should be noted that R is the blade length. The power coefficient can be seen as the blade aerodynamic efficiency which can be expressed as a nonlinear mapping (Habibi et al., 2017).

An empirical formula for C_p is often used to decrease computation time instead of a look up table that may not be generally available. An empirical formula for the power coefficient is given by (Heier, 1998),

$$C_P(\lambda,\beta) = C_1\left(\frac{C_2}{\lambda_i} - C_3\beta - C_4\right)e^{\frac{-C_5}{\lambda_i}} + C_6\lambda \quad . \qquad \frac{1}{\lambda_i} = \frac{1}{\lambda + 0.08\beta} - \frac{0.035}{\beta^3+1} \tag{2}$$

In Eq. 2 the constant coefficients are $C_1 = 0.5176$, $C_2 = 116$, $C_3 = 0.4$, $C_4 = 5$, $C_5 = 21$ and $C_6 = 0.0068$. The surface of Eq. 2 is shown in Figure 2. The maximum of C_p is 0.48 and occurs at $\beta = 0^\circ$ and $\lambda = 8.1$ (Habibi et al., 2014).

It should be noted that it is not possible to measure the wind speed at the rotor plane accurately because of spatial and temporal wind speed distributions (Esbensen et al., 2008). Therefore wind speed is considered as a disturbance on the proposed wind turbine model.

2.2. Drive Train Model

The drive train can be modelled as a two-inertia model including low speed rotor, J_r and high speed rotor, J_g. The speed ratio of the drive train gears is N_g. On the other hand, the torsion stiffness of the drive train, K_{dt} and torsion damping, B_{dt} will cause an angle of twist on the shaft, θ_Δ. The drive train efficiency is η_{dt}.

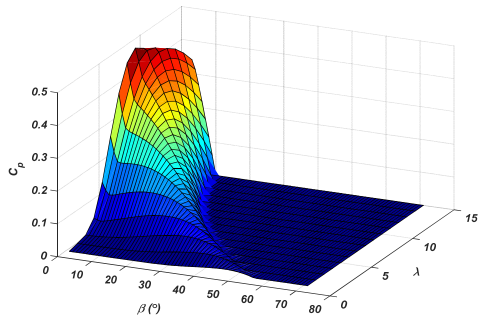

Fig. 2. The power coefficient empirical equation surface.

The transferred torque on the generator shaft is $T_g(t)$ which is rotating at the speed $\omega_g(t)$. B_r and B_g are viscous friction components of the rotor and generator shafts, respectively. The drive train model equations of motion are given as (Esbensen et al., 2008),

$$J_r\dot{\omega}_r(t) = T_a(t) - K_{dt}\theta_\Delta(t) - (B_r + B_{dt})\omega_r(t) + \frac{B_{dt}}{N_g}\omega_g(t) , \tag{3}$$

$$J_g\dot{\omega}_g(t) = \frac{\eta_{dt}K_{dt}}{N_g}\theta_\Delta(t) + \frac{\eta_{dt}B_{dt}}{N_g}\omega_r(t) - (B_g + \frac{\eta_{dt}B_{dt}}{N_g^2})\omega_g(t) - T_g(t) , \tag{4}$$

$$\dot{\theta}_\Delta(t) = \omega_r(t) - \frac{1}{N_g}\omega_g(t) . \tag{5}$$

2.3. Pitch System Model

The pitch system should track a reference value, β_{ref} and can be modelled as a first order system. It should be noted that the τ is a time constant and also t_d is the communication delay (Esbensen et al., 2008) which is as follows.

$$\dot{\beta}(t) = -\frac{1}{\tau}\beta(t) + \frac{1}{\tau}\beta_{ref}(t - t_d) . \tag{6}$$

Eq. 6 explains the operation of the pitch actuator before it has reached its limit. However, to consider a realistic model, the pitch actuator is modelled including a limited slew rate and limited operational range.

2.4. Generator and Converter Models

The extracted electrical power is produced by the generator and by controlling the current in the generator using power electronics, the variable speed feature is implemented. Accordingly, a power converter is utilized before feeding the generated electrical power into the grid and controlling the generated frequency (Sloth et al., 2011). The generator torque, $T_g(t)$, in Eq. 7 is adjusted by the reference torque $T_{g,ref}$. The converter is modelled as a first order system as follows.

$$\dot{T}_g(t) = -\frac{1}{\tau_g}T_g(t) + \frac{1}{\tau_g}T_{g,ref}(t - t_{g,d}) , \tag{7}$$

where τ_g and $t_{g,d}$ are time constant and communication delay, respectively.

It should be noted that the implemented electrical systems and controllers in the wind turbines, in terms of dynamic response, are much faster than the mechanical parts (Odgaard et al., 2013). Accordingly, the generated power, $P_g(t)$, can be approximated by (8), as a static relation, where η_g is the efficiency of the generator,

$$P_g(t) = \eta_g\omega_g(t)T_g(t) . \tag{8}$$

In addition to the delayed first order system, the generator subsystem is described by a minimum load, a maximum load, and a slew rate for the load torque.

2.5. Modelling Assumptions

The important assumptions used in the model generation are, (Wang et al., 2012; Hand et al., 2004):

- Empirical formula for power coefficient.
- The wind speed is considered as uncontrollable and unmeasurable disturbance.
- Two-inertia model of the drive train.
- First order system for pitch actuator and generator model with operational limitations for more realistic models with time constant and communication delay.
- Ignoring the yaw mechanism and assuming that the wind is always perpendicular to rotor plane.
- Wind speed covers the entire area of the rotor plane uniformly.

2.6. Assembled Model

The wind turbine model is illustrated in Figure 3, in signal low and control level. In Figure 3, the pitch system changes the pitch angle of blades based on the reference pitch angle which is applied to the turbine. This pitch angle as well as wind speed and rotor rotational speed provide the aerodynamic torque for the subsystem. This torque is applied to the drive train where the generator torque is given. The generator provides the requested electrical torque and generator reference torque to the drive train and generates the overall turbine electrical power.

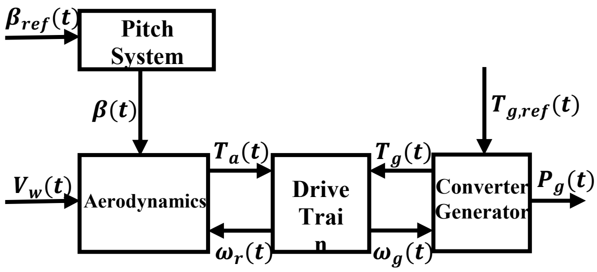

Fig. 3. Block diagram of the wind turbine model.

The available measurements from the wind turbine model are the generator and rotor speeds, generator torque and pitch angle. Also, it should be noted that generated power is calculated as per Eq. 8.

3. CONTROL STRATEGY

In the partial load operation of the wind turbine the desirable goal is to operate as close as possible to the ideal power curve, as shown in Figure 1. In partial load operation, the pitch angle of the blades are being kept at zero as the optimal value and the tip-speed ratio is held constant, i.e. $\lambda_{optimal} = 8.1$, in order to stay at the maximum C_p point. Indeed by changing the generator reference torque, $T_{g,ref}(t)$, the generator speed and rotor speed will be modified and then the tip speed ratio will achieve its optimal value to get $C_{p,\max}$ (Bianchi et al., 2006).

In partial load operation, there are two general control criteria. The first criterion is $\int P_g(t)dt$ that represents the total extracted energy. The second criteria is for the applied stress on the drive train, found by using the total torsion angle of twist of the drive train into account, that is $\int \dot{\theta}_\Delta^2(t)dt$ (Bianchi et al., 2006; Esbensen et al., 2008). Indeed, the control objective in partial load operation is to increase the total extracted energy with no significant increase in drive train stress (Esbensen et al., 2008). These criteria will be calculated for both the reference and proposed controller to evaluate the effectiveness of the new controller.

3.1. Standard Control Law (Reference Controller)

In partial load operation, the generator torque is adjusted by the electric torque controller to vary the generator speed in such a manner that the power coefficient is kept at its maximum value. The control law determines the appropriate generator torque by excluding the wind speed from aerodynamic torque, as follows (Esbensen et al., 2008),

$$T_a(t) = \frac{1}{2\omega_r(t)}\rho A\left(\frac{\omega_r(t)R}{\lambda(t)}\right)^3 C_P(\lambda(t),\beta(t)) \Rightarrow$$

$$T_a(t) = \frac{1}{2}\rho A\left(\frac{R}{\lambda(t)}\right)^3 C_P(\lambda(t),\beta(t))\omega_r^2(t), T_g(t) = \eta_{dt}\frac{T_a(t)}{N_g}$$

$$\Rightarrow T_g(t) = \frac{1}{2}\rho A\frac{\eta_{dt}R^3}{N_g^3\lambda^3(t)}C_P\omega_g^2(t) \quad . \tag{9}$$

So, based on Eq. 9, the C_P and λ tip speed ratio are set to their optimal values, i.e. $C_{P,\max} = 0.48$ and $\lambda_{opt} = 8.1$. Accordingly, Eq. 9 can be represented as,

$$T_g(t) = \underbrace{\frac{1}{2}\rho A\frac{\eta_{dt}R^3}{N_g^3\lambda_{opt}^3(t)}C_{P,\max}}_{K}\omega_g^2(t) \quad . \tag{10}$$

The function $K[Nm/(rad/s)^2]$ in Eq. 10 represents the constant gain of the standard control law. Indeed, the gain of the standard controller is computed for the optimal values of C_p and λ.

It should be noted that according to the parameters of the wind turbine model, Tables A1-A4, $K = 1.2359[Nm/(rad/s)^2]$.

The wind turbine model with the standard control law is illustrated in Figure 4. This controller is simulated to evaluate the wind turbine behaviour in section IV.

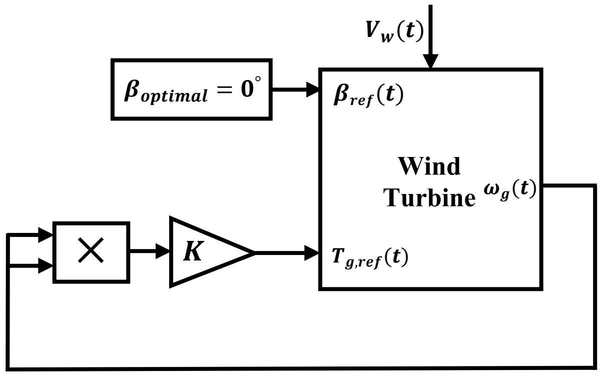

Fig. 4. The constant gain controller during partial load operation.

In this control law, the gain K is constant and there is no sense of wind variation in the control scheme. Indeed, it is obvious that the available power in the wind and consequently, the aerodynamic torque decreases when the wind speed decreases. The generator speed, ω_g, is high compared to the rotor speed which can be considered a slow dynamic system due to the large rotor inertia. For the control situation with decreasing wind speed and high ω_g, the constant gain law given by Eq. 9, still increases the $T_{g,ref}(t)$, whereas the available wind power is decreasing and so the wind turbine will consequently operate at tip speed ratios other than the optimal value. Accordingly and on simulations basis, it is shown that 20% reduction of controller gain, K, will improve the extracted power for the large wind turbines (Hand et al., 2004).

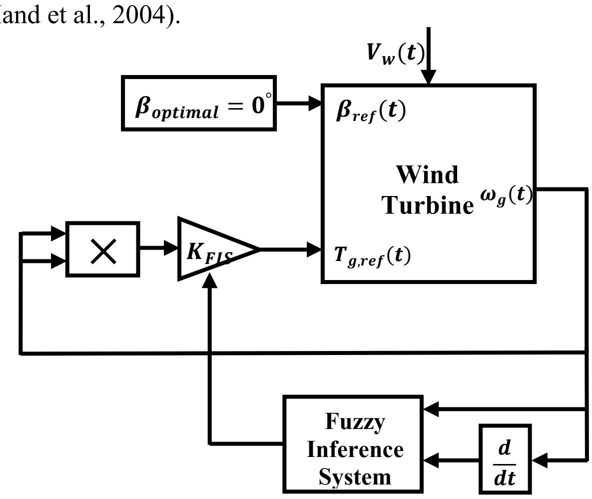

Fig. 5. The controller with fuzzy inference system (FIS).

On the other hand, as noted earlier, it is not possible to measure the wind speed variation at the rotor plane accurately.

So, in this paper it is proposed to change the controller gain based on the generator speed and its derivative using a fuzzy inference system. Figure 5 illustrates the fuzzy controlling system that is explained in the next section.

3.2. Controller with Fuzzy Inference System

Fuzzy inference system (FIS) is a nonlinear function that generates the logical output from some qualitative variables as inputs according to particular logical laws (Wang, 1999; Rebai et al., 2014; Wallam and Abbasi, 2014). This paper designs a fuzzy inference system to calculate the controller gain according to the appropriate rules, generator speed and its variation rate, as shown in Figure 5. In this proposed controller, the angular speed of the generator and its derivative are fed back to the fuzzy inference system where the controller gain is obtained based on appropriate fuzzy membership functions and fuzzy rules. Indeed, the angular speed of the generator and its derivative are used to make it possible to estimate the wind speed without the need for measuring the wind speed accurately.

An abrupt change in controller gains leads to similar changes in the reference torque and this can induce high stresses onto the drive train. So, the fuzzy membership functions of controller gain and generator speed are designed such that they change the controller gain smoothly by utilizing the Gaussian membership functions (Passino et al., 1998). These membership function are defined in Eq. 10 and are illustrated in Figures 6, 7 and 8, where μ is the membership function percentage.

$$f(x;\sigma,c)=e^{\frac{-(x-c)^2}{2\sigma^2}}, \qquad (11)$$

where x, σ and c are membership functions' range of variable, shape parameter, respectively.

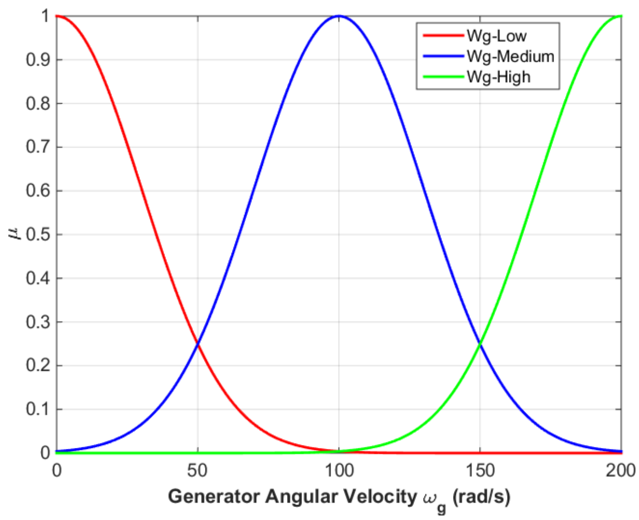

Fig. 6. The fuzzy membership functions of ω_g. The red, blue and green curves are named as low, medium and high membership functions for ω_g, respectively.

It should be noted that only the sign of the generator speed derivative, $\dot{\omega}_g$, is of interest to consider the generator speed variation. Therefore, the $\dot{\omega}_g$ membership functions are designed to be small to represent only the sign by selecting small σ in the Gaussian membership function (Passino et al., 1998), as shown in Figure 7. The inputs of FIS are ω_g and its derivative and the output of FIS is the controller gain. The initial values are as given in Table 1.

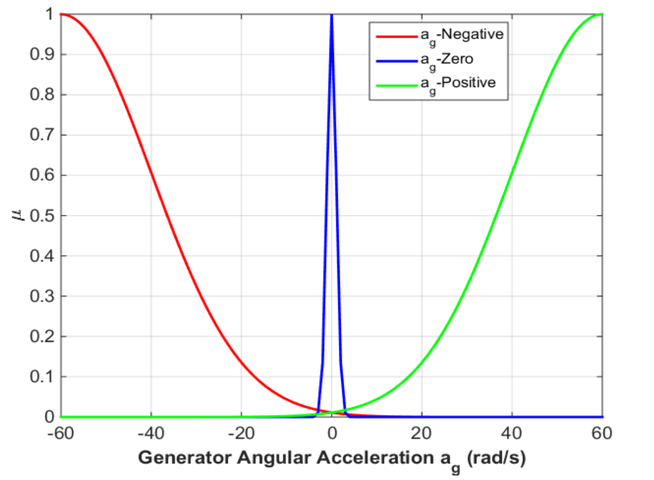

Fig. 7. The fuzzy membership functions of $\dot{\omega}_g$. The red, blue and green curves are named as negative, zero and positive membership functions for $\dot{\omega}_g$, respectively.

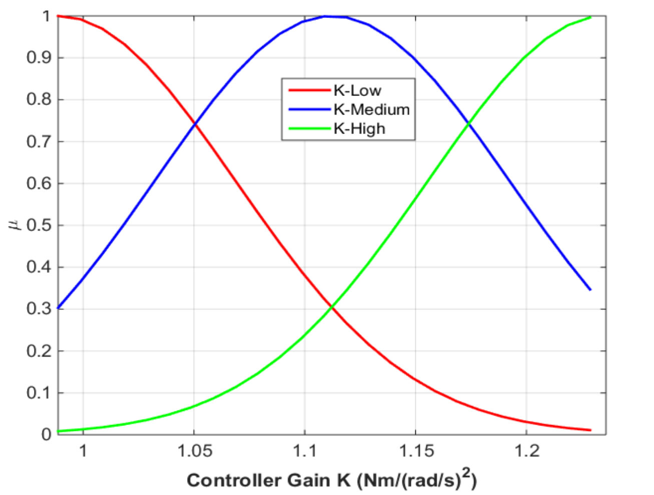

Fig. 8. The fuzzy membership functions of controller gain. The red, blue and green curves are named as low, medium and high membership functions for controller gain, respectively.

The fuzzy rules are defined with respect to the idea of adjusting the controller gains based on wind speed variation. This idea is obtained from the wind turbine behaviour as a high inertia mechanism. This behaviour can be summarized as: whenever the wind speed has an increasing high value, the ω_g will be high and $\dot{\omega}_g$ will be positive and vice versa. On the other hand the sign of $\dot{\omega}_g$ and value of ω_g represent the variation and value of wind speed, respectively. So ω_g and $\dot{\omega}_g$ can be used to determine the behaviour of wind speed.

Table 1. Initial values for fuzzy membership functions.

Initial Membership Functions of Generator Angular Velocity $\omega_g(t)$	Parameters	
	σ	c
Low	30	0
Medium	30	100
High	30	200
Initial Membership Functions of Controller Gain K	Parameters	
	σ	c
Low	0.08	0.9887
Medium	0.08	1.1123
High	0.08	1.2356
Initial Membership Functions of Generator Angular Acceleration $\dot{\omega}_g(t)$	Parameters	
	σ	c
Negative	20	-60
Zero	1	0
Positive	20	60

The controller gain can be tuned based on wind speed and its variation, as discussed earlier. In this paper it is proposed to use ω_g and $\dot{\omega}_g$ instead of wind speed, because, irrespective of the wind speed, these two signals are measurable in wind turbines. Therefore whenever ω_g is high and $\dot{\omega}_g$ is positive, i.e. wind speed is an increasing high value, there is high power content and the wind turbine should extract as much power as possible. This can be done by increasing the controller gain that leads to increasing $T_{g,ref}(t)$. On this basis, the fuzzy rules are defined and shown in Table 2.

Table 2. Fuzzy rules.

		Generator Angular Velocity ω_g		
		Low	Medium	High
Generator Angular Acceleration $\dot{\omega}_g$	Negative	Low Gain	Low Gain	Medium Gain
	Zero	Low Gain	Medium Gain	High Gain
	Positive	Medium Gain	High Gain	High Gain

The Mamdani inference engine is one of the most appropriate engines for control processes (Passino et al., 1998). Therefore this inference engine is used to complete the fuzzy inference system, shown as a curve in Figure 9.

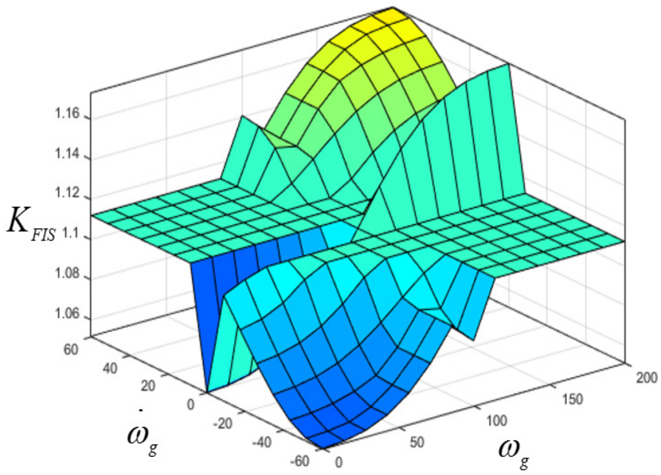

Fig. 9. The fuzzy inference system curve.

In Figure 9, all membership functions, Figure 6, 7 and 8, are combined according to fuzzy rules which are defined in Table 2. This curve shows the nonlinear mapping from ω_g and $\dot{\omega}_g$ to K_{FIS}. This mapping calculates the appropriate controller gain for the proposed fuzzy controller.

4. SIMULATION RESULTS

The wind speed for designing the fuzzy controller is shown in Figure 10 (Bianchi et al., 2006), and accordingly, the simulation results are investigated in Matlab/Simulink for both reference controller and fuzzy controller.

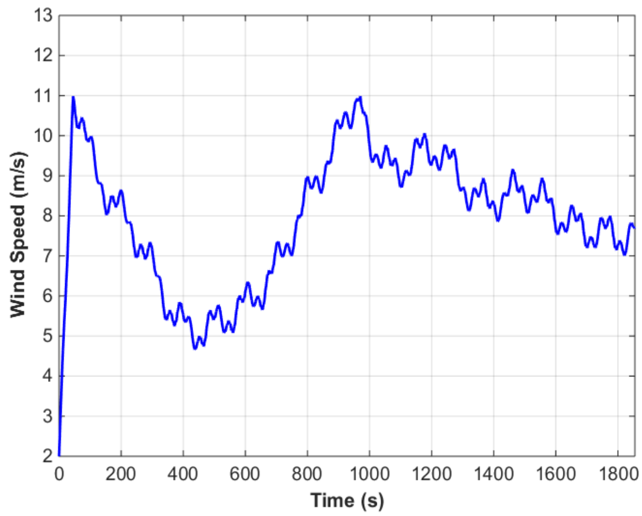

Fig. 10. Wind speed signal.

4.1. Reference Controller Results

The tip speed ratio and power coefficient are shown in Figures 11 and 12, respectively. It is obvious that the constant controller gain, after the transient response, is trying to keep the tip speed ratio and power coefficient at their optimal values.

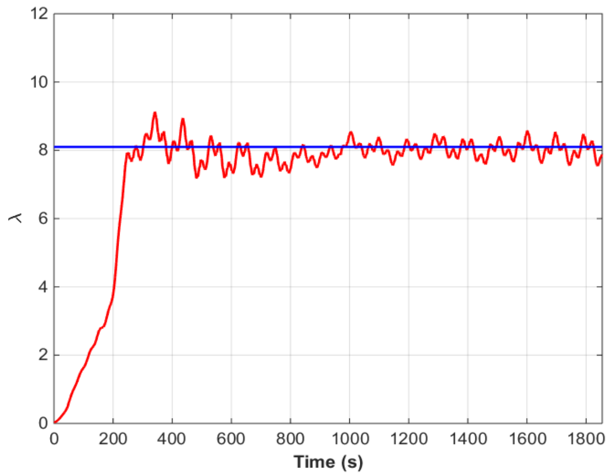

Fig. 11. Comparison of tip speed ratio of reference controller (red line) with optimal value (blue line).

It is obvious from Figure 10 that whenever the wind speed changes abruptly, the tip speed ratio and power coefficient, Figures 11 and 12, deviates from optimal values. The generated power of the wind turbine with the reference controller is shown in Figure 13.

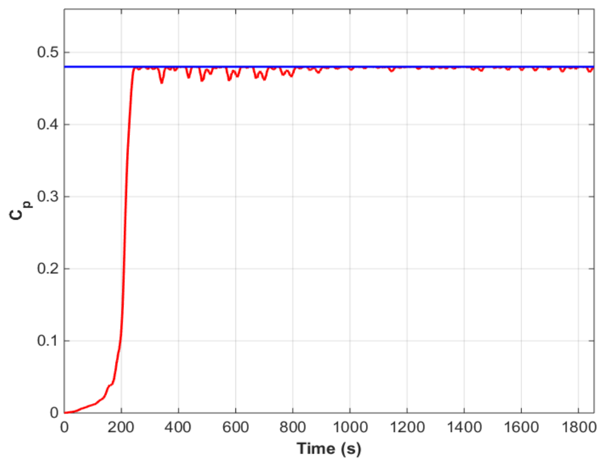

Fig. 12. Comparison of power coefficient of reference controller (red line) with optimal value (blue line).

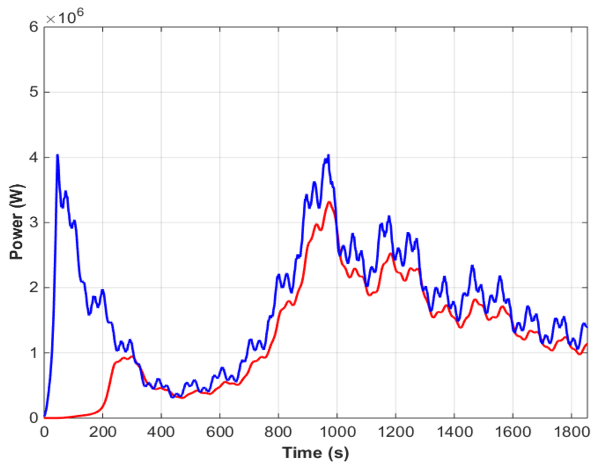

Fig. 13. Comparison of power of reference controller (red line) with optimal value (blue line).

The ideal power tracking ability, as the main controller objective, is obvious in Figure 13. The two control criteria that have been described previously, are used to quantify controller tasks and compared with the fuzzy controller response to evaluate the effectiveness of proposed controller. The values of the two control criteria for reference, are given in Table 3.

Table 3. Values of two control criteria for reference controller.

$\int P_g(t)dt$	$\int \dot{\theta}_\Delta^2(t)dt$
$2.316\times10^9\, J$	$9.906\times10^{-9}\,\frac{rad^2}{s}$

4.2. Fuzzy Inference System Controller Results

Firstly, the procedure for designing the proposed fuzzy controller and membership functions are considered and then after comparison between various memberships shape functions, the ones that produce the most energy are selected. It should be noted that changing the controller gain abruptly makes the drive train to increase or decrease velocity very fast and consequently, the stress on the drive train will be increased. Therefore, to change the controller gains smoothly the Gaussian membership functions are chosen.

The Gaussian membership functions, Eq. 10, depend on x, σ and c that are range of variable, shape parameter and centre of membership functions, respectively. A range of values were considered as fuzzy inputs and outputs and in order to reduce the simulation time, three membership functions for each variable were selected so that their centres were located at the beginning, the middle and at the end of their range. Accordingly, the shape and operation of the fuzzy controller depends on the σ of each membership function.

Some initial values of σ for each membership function were selected as given in Table 1, and then the extracted energy and corresponding stress on the drive train were calculated as shown in Table 4.

Table 4. Values of two control criteria for the fuzzy controller with initial values for membership functions.

$\int P_g(t)dt$	$\int \dot{\theta}_\Delta^2(t)dt$
$2.328\times10^9\, J$	$9.864\times10^{-9}\,\frac{rad^2}{s}$

Even with the initial membership function, comparison of the results in Tables 2 and 3 shows that the extracted energy was increased by 0.52 % while the drive train stress was decreased. Indeed, the captured power using the fuzzy controller is closer to the ideal power curve compared to the reference controller. High drive train stress results in unpredictable maintenance procedures and increases the shutdown period of the wind turbine and consequently, increases the operational and lifetime costs. The proposed fuzzy controller has increased the total extracted energy with no considerable increase in drive train stress. Therefore the overall energy cost can be decreased.

The tip speed ratio, power coefficient and generated power when using the fuzzy controller with initial values are shown in Figures 14, 15 and 16.

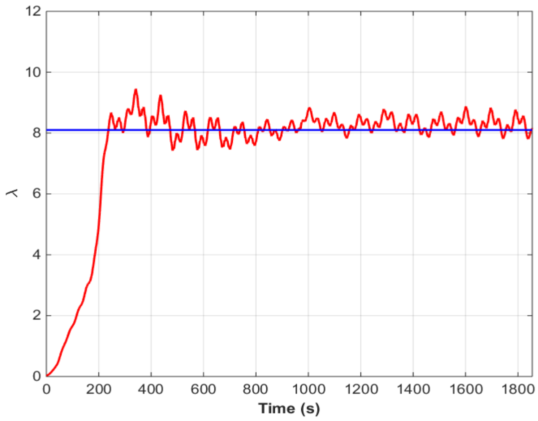

Fig. 14. Comparison of tip speed ratio of fuzzy controller with initial values (red line) with optimal value (blue line).

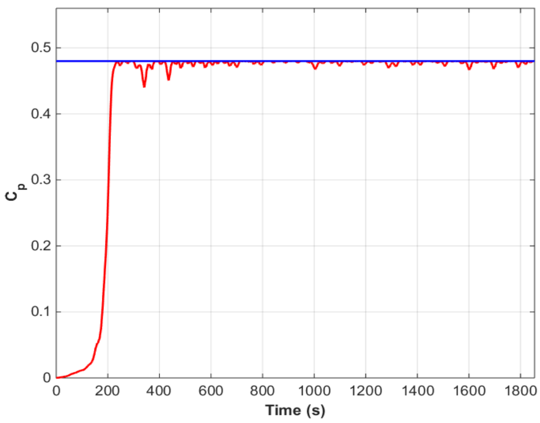

Fig. 15. Comparison of power coefficient of fuzzy controller with initial values (red line) with optimal value (blue line).

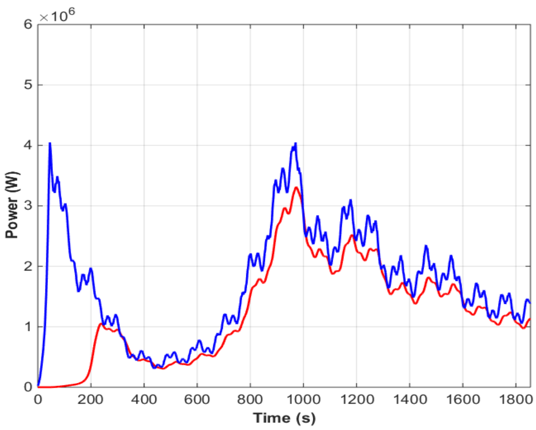

Fig. 16. Comparison of power of fuzzy controller (red line) with optimal value (blue line).

By changing the values of σ for each membership function, the effect of membership functions on the extracted energy and control criteria can be studied and the membership functions that generate the most energy can be chosen.

Firstly, the membership functions of ω_g are considered. It should be noted that the centre of membership functions of ω_g are fixed on 0, 100 and 200 for Low, Medium and High membership functions, respectively. It should be noted that because of the nonlinear wind turbine model and the structure of the fuzzy inference system, it was not possible to find the best σ of membership functions automatically via simulation, because in each step the designed fuzzy controller should be updated and implemented in the wind turbine model. Thus a step by step trial and error procedure was used to find the best fuzzy controller.

In the first step, the σ of three membership functions of ω_g were changed in the same manner. The results are summarized in Table 5. Additionally, membership functions of K and $\dot{\omega}_g(t)$ are the same as Table 1. In Table 5, σ_L, σ_M and σ_H stand for σ of Low, Medium and High membership functions of ω_g, respectively.

It is obvious that when σ is 26.875, the most energy is extracted. It should be noted that the σ of membership functions of K and $\dot{\omega}_g$, throughout Tables 5-7, are fixed at their initial values.

Table 5. Fuzzy controller criteria values, σ of ω_g membership functions are changed.

σ_L	σ_M	σ_H	Energy	Stress
10	10	10	2.324e9	9.745e-9
20	20	20	2.327e9	9.848e-9
22.5	22.5	22.5	2.328e9 (2327692836.4794)	9.861e-9
25	25	25	2.328e9 (2327911944.8145)	9.867e-9
25.625	25.625	25.625	2.328e9 (2327936089.9828)	9.868e-9
26.25	26.25	26.25	2.328e9 (2327949150.3805)	9.868e-9
26.875	26.875	26.875	2.328e9 (232796089.9828)	9.868e-9
27.5	27.5	27.5	2.328e9 (2327944464.4127)	9.868e-9
28.75	28.75	28.75	2.328e9 (2327903022.4433)	9.866e-9
35	35	35	2.327e9	9.848e-9
40	40	40	2.327e9	9.839e-9
50	50	50	2.326e9	9.854e-9
60	60	60	2.326e9	9.883e-9

Now, because it is necessary to increase controller gain at high ω_g as much as to decrease controller gain at low ω_g, the membership functions of ω_g_Low and ω_g_High were selected to be the same as each other while ω_g_Medium can be different. So, at this step σ_L and σ_H are changed and σ_M was fixed at 26.875 to check if it was possible to increase the extracted energy compared to the previous step. The results are summarized in Table 6.

When σ_L and σ_H are 70, it can be seen that the most energy is extracted. Now by holding σ_L and σ_H constant at 70, the σ_M was again changed as shown in Table 7.

Table 6. Fuzzy controller criteria values, σ_L and σ_H of ω_g membership functions are changed, σ_M is fixed at 26.875.

σ_L	σ_M	σ_H	Energy	Stress
10	26.875	10	2.324e9	1.021e-8
30	26.875	30	2.328e9	0.989e-8
40	26.875	40	2.329e9	1.010e-8
50	26.875	50	2.329e9	1.022e-8
60	26.875	60	2.330e9 (2330313904.1584)	1.032e-8
65	26.875	65	2.330e9 (2330498207.3282)	1.038e-8
67.5	26.875	67.5	2.330e9 (2330565528.4886)	1.037e-8
68.75	26.875	68.75	2.330e9 (2330585510.9175)	1.037e-8
70	26.875	70	2.330e9 (2330595389.6470)	1.038e-8
71.25	26.875	71.25	2.330ee (2330595120.3822)	1.037e-8
72.5	26.875	72.5	2.330e9 (2330585339.7532)	1.389e-8
75	26.875	75	2.330e9 (2330539459.351)	1.039e-8
80	26.875	80	2.330e9 (2330356100.9071)	1.039e-8

Table 7. Fuzzy controller criteria values, σ_L and σ_H of ω_g membership functions are fixed at 70, σ_M is changed.

σ_L	σ_M	σ_H	Energy	Stress
70	1	70	2.332e9 (2332635598.3994)	1.069e-8
70	1.25	70	2.332e9 (2332636401.0613)	1.066e-8
70	1.875	70	2.332e9 (2332631863.8027)	1.065e-8
70	2.5	70	2.332e9 (2332613369.0814)	1.064e-8
70	3.75	70	2.332e9 (2332603145.6117)	1.065e-8
70	5	70	2.332e9 (2332577019.2552)	1.064e-8
70	7.5	70	2.332e9 (2332533538.1301)	1.069e-8
70	10	70	2.332e9 (2332426649.9962)	1.074e-8
70	20	70	2.331e9	1.068e-8
70	40	70	2.327e9	1.003e-8

It can be concluded that when σ_M is 1.25 and σ_L and σ_H are 70 most energy is extracted.

Now by holding these values for membership functions of $\omega_g(t)$ the extracted energy can be further improved by changing the membership functions of K. Additionally, membership functions of $\dot{\omega}_g(t)$ were fixed at initial values as given in Table 1. It should be noted that the centre of membership functions of K were fixed at 0.9887, 1.1123 and 1.2356 for Low, Medium and High membership functions of K, respectively. Using the same procedure as for ω_g, the σ for these three membership functions were changed in the same manner. The results are shown in Table 8 where σ_L, σ_M and σ_H stand for σ of Low, Medium and High membership functions of K, respectively.

It should be noted that the σ of membership functions of $\omega_g(t)$ and $\dot{\omega}_g$, throughout Tables 8-10, are fixed at the highlighted ones in Table 7 and at their initial values, respectively.

Table 8. Fuzzy controller criteria values, σ of K membership functions are changed.

σ_L	σ_M	σ_H	Energy	Stress
0.0015	0.0015	0.0015	2.337e9 (2337408691.3984)	1.116e-8
0.002	0.002	0.002	2.337e9 (2337791496.6786)	1.115e-8
0.0025	0.0025	0.0025	2.337e9 (2337470995.2073)	1.112e-8
0.004	0.004	0.004	2.337e9 (2337223138.6927)	1.110e-8
0.005	0.005	0.005	2.337e9 (2337104898.2222)	1.108e-8
0.0075	0.0075	0.0075	2.336e9	1.112e8
0.01	0.01	0.01	2.336e9	1.102e-8
0.015	0.015	0.015	2.336e9	1.098e-8
0.02	0.02	0.02	2.335e9	1.094e-8
0.04	0.04	0.04	2.334e9	1.083e-8
0.05	0.05	0.05	2.334e9	1.077e-8
0.07	0.07	0.07	2.333e9	1.070e-8
0.1	0.1	0.1	2.331e9	1.051e-8
0.12	0.12	0.12	2.329e9	1.032e-8

When σ_L, σ_M and σ_H are 0.002, the most energy is extracted. Now by holding σ_M constant at 0.002, the σ_L and σ_H were further changed as shown in Table 9 to increase the extracted energy.

Table 9. Fuzzy controller criteria values, σ_L and σ_H of K membership functions are changed, σ_M is fixed at 0.002.

σ_L	σ_M	σ_H	Energy	Stress
0.00025	0.002	0.00025	2.338e9 (2338970041.5241)	1.134e-8
0.0005	0.002	0.0005	2.338e9 (2.338969950.1375)	1.134e-8
0.001	0.002	0.001	2.337e9	1.113e-8
0.0015	0.002	0.0015	2.337e9	1.117e-8
0.003	0.002	0.003	2.337e9	1.118e-8
0.004	0.002	0.004	2.337e9	1.114e-8
0.005	0.002	0.005	2.337e9	1.113e-8

When σ_L and σ_H are 0.00025 and σ_M is 0.002, the most energy is extracted. Consequently, keeping the value 0.00025 for σ_L and σ_H, the σ_M was further changed as shown in Table 10. It can be seen that when σ_M is 0.0005 and σ_L and σ_H are 0.00025, the most energy was extracted. Now by holding these values for membership functions of K the extracted energy will be further improved by changing the membership functions of $\dot{\omega}_g(t)$. It should be noted that the centre of membership functions of $\dot{\omega}_g(t)$ are fixed on -60, 0 and 60 for Negative, Zero and Positive membership functions of $\dot{\omega}_g(t)$, respectively.

Table 10. Fuzzy controller criteria values, σ_L and σ_H of K membership functions are fixed at 0.00025, σ_M is changed.

σ_L	σ_M	σ_H	Energy	Stress
0.00025	0.0005	0.00025	2.339e9 (2339687964.1884)	1.144e-8
0.00025	0.001	0.00025	2.339e9 (2339338165.3230)	1.139e-8
0.00025	0.0015	0.00025	2.339e9 (2339185861.5889)	1.137e-8
0.00025	0.004	0.00025	2.338e9	1.123e-8

Firstly, σ of Negative and Positive membership functions were changed in the same manner and σ of Zero membership function was held at its initial value. The results are summarized in Table 11, where σ_N, σ_Z and σ_P stand for σ of Negative, Zero and Positive membership functions of $\dot{\omega}_g(t)$, respectively.

It should be noted that the σ of membership functions of $\omega_g(t)$ and K, throughout Tables 11 and 12, are fixed at the highlighted ones in Tables 7 and 10, respectively.

When σ_N and σ_P are 5 and σ_Z is 1, the most energy was extracted. Consequently, keeping the value of 5 for σ_N and σ_P, the σ_Z was further changed as shown in Table 12, to improve the extracted energy. Evidently, when σ_N, σ_Z and σ_P are 5, 10 and 5, respectively, the most energy was extracted. Finally, all membership functions that generate the most energy and the corresponding extracted energy and the estimated stress are summarized in Table 13 and 14, respectively.

Table 11. Fuzzy controller criteria values, σ_N and σ_P of $\dot{\omega}_g$ membership functions are changed, σ_Z is fixed at initial value.

σ_N	σ_Z	σ_P	Energy	Stress
2	1	2	2.339e9 (2339866196.7744)	1.147e-8
5	1	5	2.339e9 (2339866196.7744)	1.147e-8
7	1	7	2.339e9 (2339866196.7744)	1.147e-8
10	1	10	2.339e9 (2339866195.9149)	1.147e-8
15	1	15	2.339e9 (2339859363.6174)	1.147e-8
40	1	40	2.335e9	1.099e-8

Table 12. Fuzzy controller criteria values, σ_N and σ_P of $\dot{\omega}_g$ membership functions are fixed at 5, σ_Z is changed.

σ_N	σ_Z	σ_P	Energy	Stress
5	0.5	5	2.336e9	1.149e-8
5	3	5	2.340e9 (2339993521.5462)	1.151e-8
5	5	5	2.340e9 (2339993533.7857)	1.151e-8
5	10	5	2.340e9 (2339993533.7981)	1.151e-8
5	15	5	2.340e9 (2339993533.7981)	1.151e-8

Table 13. Best values for fuzzy membership functions.

Best Membership Functions of Generator Angular Velocity $\omega_g(t)$	Parameters σ	Parameters c
Low	70	0
Medium	1.25	100
High	70	200
Best Membership Functions of Controller Gain K	**σ**	**c**
Low	0.00025	0.9887
Medium	0.0005	1.1123
High	0.00025	1.2356
Best Membership Functions of Generator Angular Acceleration $\dot{\omega}_g(t)$	**σ**	**c**
Negative	5	-60
Zero	10	0
Positive	5	60

It is obvious that the extracted energy is increased by 1.03 % with proposed fuzzy controller whilst there was a 16 % increase in total stress.

Now to consider the applicability of the proposed controller, a real measured wind speed (Odgaard and Stoustrup, 2015), shown in Figure 17, is used as a disturbance on the nonlinear model of the wind turbine. The results are summarized in Table 15.

Table 14. Comparison of two control criteria values for all controllers.

	$\int P_g(t)dt$	$\int \dot{\theta}_\Delta^2(t)dt$
Reference (Constant Gain) Controller	$2.316\times10^9 J$	$9.906\times10^{-9}\ \frac{rad^2}{s}$
Fuzzy Controller with initial values for membership functions	$2.328\times10^9 J$	$9.864\times10^{-9}\ \frac{rad^2}{s}$
Fuzzy Controller with best values for membership functions	$2.340\times10^9 J$	$1.151\times10^{-8}\ \frac{rad^2}{s}$

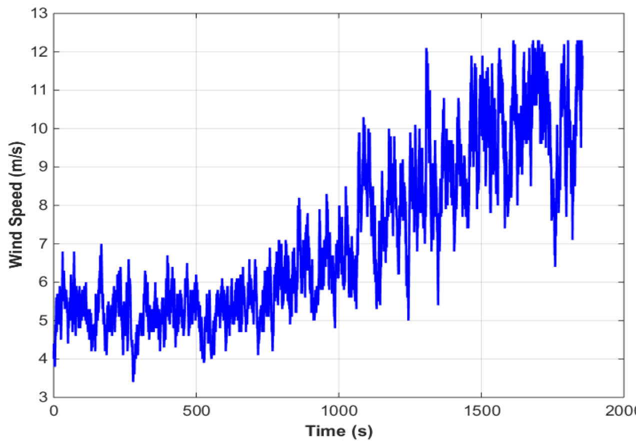

Fig. 17. Real Wind speed sigSnal, (Odgaard and Stoustrup, 2015).

Table 15. Comparison of two control criteria values for all controllers with real wind speed.

	$\int P_g(t)dt$	$\int \dot{\theta}_\Delta^2(t)dt$
Reference (Constant Gain) Controller	$1.93\times10^9 J$	$5.919\times10^{-6}\ \frac{rad^2}{s}$
Fuzzy Controller with initial values for membership functions	$1.944\times10^9 J$	$8.082\times10^{-6}\ \frac{rad^2}{s}$
Fuzzy Controller with best values for membership functions	$1.952\times10^9 J$	$6.271\times10^{-6}\ \frac{rad^2}{s}$

It is obvious that with the proposed fuzzy controller, for the real wind speed, the extracted energy is increased about 1.13 % with a consequential 6 % increase in total drive train stress. These results show the effectiveness of using the nonlinear fuzzy logic controller to model the extracted energy and drive train stress in partial load operation. Tuning of the controller shows the important ability to maximize extracted energy while modelling the resulting changes of drive train stress.

5. CONCLUSION

This paper presents an analysis of the potential improvement of the partial load operation of a 4.8 MW wind turbine using a fuzzy inference system to track the ideal power curve as close as possible. With the use of the standard reference controller, the extracted power was obtained to study the behaviour of the wind turbine. In partial load operation, the fuzzy control strategy aims to stay at the maximum power coefficient. The maximum power coefficient occurs at a given pitch angle and tip speed ratio. Thus, by defining fuzzy rules with control of generator speed, the modified controller gain was obtained. The total harvested energy of wind turbine, was shown to be increased by 1.13% using proposed controller. This value for an industrial wind turbine is a desirable improvement. It should be noted that the total energy was increased with a 6 % increase to the drive train stress. This improvement in extracted energy can reduce the cost of generated power provided it does not significantly affect the system reliability.

Additionally, the fuzzy inference controller was implemented on the nonlinear model and the wind turbine model was not linearized. The proposed fuzzy controller should be practical for real wind turbines where all available fuzzy membership functions can be implemented to provide the choice of controller to harvest more energy from the wind speed. The applicability and generality of the proposed controller was tested with a real wind speed signal that was modelled as a disturbance input.

REFERENCES

Aissaoui, A. G., Tahour, A., Essounbouli, N., Nollet, F., Abid, M. & Chergui, M. I. (2013). A Fuzzy-PI control to extract an optimal power from wind turbine. *Energy Conversion and Management*, 65, 688-696.

Ata, R. & Koçyigit, Y. (2010). An adaptive neuro-fuzzy inference system approach for prediction of tip speed ratio in wind turbines. *Expert Systems with Applications*, 37(7), 5454-5460.

Badihi, H., Zhang, Y. & Hong, H. (2014). Fuzzy gain-scheduled active fault-tolerant control of a wind turbine. *Journal of the Franklin Institute*, 351(7), 3677-3706.

Bedoud, K., Ali-Rachedi, M., Bahi, T. & Lakel, R. (2015). Adaptive Fuzzy Gain Scheduling of PI Controller for control of the Wind Energy Conversion Systems. *Energy Procedia*, 74, 211-225.

Bianchi, F. D., De Battista, H. & Mantz, R. J. (2006). *Wind turbine control systems: principles, modelling and gain scheduling design*. Springer Science & Business Media.

Bououden, S., Filali, S. & Chadli, M. (2013). Fuzzy Predictive Control of a Variable Speed Wind Turbine. *Energy Procedia*, 42, 357-366.

Esbensen, T., Jensen, B., Niss, M., Sloth, C. & Stoustrup, J. (2008). *Joint power and speed control of wind turbines*. Aalborg University, Aalborg, 120.

Gao, F., Xu, D. & Lv, Y. (2008). Pitch-control for large-scale wind turbines based on feed forward fuzzy-PI. *IEEE 7th World Congress on Intelligent Control and Automation (WCICA)*, 2277-2282.

Habibi, H., Koma, A. Y., & Sharifian, A. (2016). Power and velocity control of wind turbines by adaptive fuzzy controller during full load operation. *Iranian Journal of Fuzzy Systems*, 13(3), 35-48.

Habibi, H., Rahimi Nohooji, H., & Howard, I. (2017). Power maximization of variable-speed variable-pitch wind turbines using passive adaptive neural fault tolerant control. *Frontiers of Mechanical Engineering*, 1-12. doi:10.1007/s11465-017-0431-4

Habibi, H., & Yousefi-Koma, A. (2014). Increase of Extracted Energy of a Wind Turbine in Partial load Operation. *10th international Energy Conference (IEC 2014)*, Tehran, Iran, 1-10.

Hammerum, K. (2006). *A fatigue approach to wind turbine control*. Technical University of Denmark, DTU, DK-2800 Kgs. Lyngby, Denmark.

Hand, M., Johnson, K., Fingersh, L. & Wright, A. (2004). *Advanced control design and field testing for wind turbines at the National Renewable Energy Laboratory*. National Renewable Energy Lab., Golden, CO, NREL/CP-500-36118.

Heier, S. (1998). Grid integration of wind energy conversion systems, Wiley.

Jian-Jun, X., Li-Mei, Y., Xiao-Ning, Q., Chun-Lei, J. & Jian-Ren, W. (2010). Study of variable-pitch wind turbine based on fuzzy control. *IEEE 2nd International Conference on Future Computer and Communication (ICFCC)*, V1-235-V1-239.

Johnson, K. E., Pao, L. Y., Balas, M. J. & Fingersh, L. J. (2006). Control of variable-speed wind turbines: standard and adaptive techniques for maximizing energy capture. *Control Systems*, 26(3), 70-81.

Lajouad, R., Magri, A. E., Fadili, A. E., Chaoui, F. Z. & Giri, F. (2014). Adaptive Nonlinear Control of Wind Energy Conversion System Involving Induction Generator. *Asian Journal of Control*, 17(4), 1365–1376.

Lakhal, Y., Baghli, F. Z. & El Bakkali, L. (2015). Fuzzy Logic Control Strategy for Tracking the Maximum Power Point of a Horizontal Axis Wind Turbine. *Procedia Technology*, 19, 599-606.

Laks, J. H., Pao, L. Y. & Wright, A. D. (2009). Control of wind turbines: Past, present, and future. *American Control Conference (ACC'09)*, 2096-2103.

Odgaard, P. F. & Stoustrup, J. (2015). A benchmark evaluation of fault tolerant wind turbine control concepts. *IEEE Transactions on Control Systems Technology*, 23(3), 1221-1228.

Odgaard, P. F., Stoustrup, J. & Kinnaert, M. (2013). Fault-tolerant control of wind turbines: A benchmark model. *IEEE Transactions on Control Systems Technology*, 21(4), 1168-1182.

Passino, K. M., Yurkovich, S. & Reinfrank, M. (1998). *Fuzzy control*. 42. Citeseer.

Qi, Y. & Meng, Q. (2012). The application of fuzzy PID control in pitch wind turbine. *Energy Procedia*, 16, 1635-1641.

Rebai, A., Guesmi, K., Gozim, D. & Hemici, B. (2014). Design of an optimized fractional order fuzzy PID controller for a piezoelectric actuator. *IEEE 15th International Conference on Sciences and Techniques of Automatic Control and Computer Engineering (STA)*, 456-461.

Shamshirband, S., Petković, D., Ćojbašić, Ž., Nikolić, V., Anuar, N. B., Shuib, N. L. M., Kiah, M. L. M. & Akib, S. (2014). Adaptive neuro-fuzzy optimization of wind farm project net profit. *Energy Conversion and Management*, 80, 229-237.

Sloth, C., Esbensen, T., Niss, M. O., Stoustrup, J. & Odgaard, P. F. (2009) Robust LMI-based control of wind turbines with parametric uncertainties. *IEEE Control Applications (CCA) & Intelligent Control (ISIC)*, 776-781.

Sloth, C., Esbensen, T. & Stoustrup, J. (2011). Robust and fault-tolerant linear parameter-varying control of wind turbines. *Mechatronics*, 21(4), 645-659.

Wallam, F. & Abbasi, A. R. (2014). Evaluating the transient handling capability of a fuzzy logic controller for a pressurized heavy water reactor. *Control engineering and applied informatics*, 16(2), 40-48.

Wang, H., Pintea, A., Christov, N., Borne, P. & Popescu, D. (2012). Modelling and recursive power control of horizontal variable speed wind turbines. *Journal of Control Engineering and Applied Informatics*, 14(4), 33-41.

Wang, L. X. (1999). *A course in fuzzy systems*, Prentice-Hall press, USA.

APPENDIX

Tables A1-A4 show the value of parameters used in wind turbine modelling (Habibi et al., 2016).

Table A1. Aerodynamic.

Parameter	Swept Area (A)	Blade Length (R)	Air Density (ρ)
Value	10387 [m^2]	57.5 [m]	1.225 [kg/m^3]

Table A2. Generator Model

Parameter	Value
Time Constant of The First Order System (τ_g)	20 [ms]
Communication Delay of The Converter ($t_{g,d}$)	10 [ms]
Minimum Generator Torque Variation Rate ($\dot{T}_{g,\min}$)	-50 [MNm/s]
Maximum Generator Torque Variation Rate ($\dot{T}_{g,\max}$)	50 [MNm/s]
Minimum Possible Generator Torque ($T_{g,\min}$)	0 [Nm]
Maximum Possible Generator Torque ($T_{g,\max}$)	35000 [Nm]
Minimum Generator Power ($P_{g,\min}$)	0 [W]
Maximum Generator Power ($P_{g,\max}$)	5.3 [MW]

Table A3. Pitch Actuator

Parameter	Value
Time Constant of The First Order System (τ)	50 [ms]
Communication Delay of The Pitch Actuator (t_d)	10 [ms]
Minimum Pitch Angle Variation Rate ($\dot{\beta}_{\min}$)	-10 [°/s]
Maximum Pitch Angle Variation Rate ($\dot{\beta}_{\max}$)	10 [°/s]
Minimum Pitch Angle ($\beta_{\min}$)	-10 [°]
Maximum Pitch Angle ($\beta_{\max}$)	40 [°]

Table A4. Drive Train Model

Parameter	Value
Torsion Damp Coefficient (B_{dt})	9.45 [$MNm/(rad/s)$]
Friction of the Generator Shaft (B_g)	3.034 [$Nm/(rad/s)$]
Friction of the Rotor Shaft (B_r)	27.8 [$KNm/(rad/s)$]
Inertia of the Generator Shaft (J_g)	390 [kgm^2]
Inertia of the Rotor Shaft (J_r)	55 [$Mkgm^2$]
Torsion Stiffness (K_{dt})	2.7 [GNm/rad]
Gear Ratio (N_g)	95
Efficiency (η_{dt})	0.97